Biophysical Chemistry 15 (1981) 53–64
Elsevier Biomedical Press

THE pH-DEPENDENT STRUCTURE OF CALF THYMUS DNA STUDIED BY RAMAN SPECTROSCOPY

T. O'CONNOR *, S. MANSY **, M. BINA, D.R. McMILLIN, M.A. BRUCK *** and R.S. TOBIAS †

Department of Chemistry, Purdue University, West Lafayette, IN 47907, U.S.A.

Received 12th August 1981

Key words: Raman spectroscopy; DNA denaturation; DNA structure; C-form DNA

The pH-dependent structure of calf thymus DNA is analyzed using Raman spectroscopy. The Raman spectra in the acidic region demonstrate that denaturation occurs in several steps. The binding of H^+ to adenine and cytosine residues is accompanied by a decrease in the percentage of DNA in the B-conformation and a concurrent increase in a conformation most probably related to the C-form. The denaturation of DNA is observed at pH 3.3 and parallels the protonation of guanine bases. The Raman spectra of calf thymus DNA in the basic region (above pH 10) show that guanine residues are deprotonated at a lower pH value than are thymine residues. In addition, Raman spectra in the basic region detect conformational changes of the phosphate backbone different from those found in the acidic region.

1. Introduction

Our group [1–4] and others [4–12] have used Raman spectroscopy to study the molecular vibrations of polynucleotides in order to obtain detailed structural information. Since H^+ behaves as an electrophile, studies of structure as a function of pH provide data to aid the interpretation of electrophilic attack on nucleic acids. We have previously demonstrated that Raman difference spectroscopy is an important probe of metal electrophile binding to nucleic acids [1–3]. Therefore, Raman and Raman difference spectroscopy can be used to monitor several different features associated with DNA structure that include protonation and deprotonation sites, base stacking, and backbone conformation [5–7,9,10,12].

In other investigations, Erfurth and Peticolas [6] and Rimai et al. [5] have followed the thermal denaturation of DNA with Raman spectroscopy. Raman spectroscopy, however, is not limited to the investigation of denaturation, but can also monitor premelting effects in double-stranded DNAs [6], double-stranded RNAs [4] and single-stranded RNAs [11]. Additionally, comparison of X-ray diffraction patterns and Raman spectra of DNA fibers have given fingerprint spectra for different DNA backbone conformations [7]. Therefore, the appearance of a characterized DNA form can be tracked by Raman spectroscopy.

This report examines the pH-dependent structure of DNA between pH 2.35 and 11.87. Our detailed analysis of the pH-dependent structure of DNA by Raman spectroscopy complements and extends studies that used other techniques [8,13–19].

* Present address: Department of Biochemistry, University of Wisconsin-Madison, 420 Henry Mall, Madison, WI 53706, U.S.A.
** Present address: Sharon Woods Technical Center, Procter and Hartman Highway, Cinncinati, OH 45241, U.S.A.
*** Present address: Department of Chemistry, University of Southern California, Los Angeles, CA 90007, U.S.A.
† Deceased, February 1980.

0301-4622/0000–0000/$02.75

2. Experimental

2.1. Sample preparation

The nucleotide and DNA model solutions were prepared using 5'-ribonucleotides obtained from either Sigma Chemical Co., St. Louis, MO, or PL Biochemicals, Milwaukee, WI. The individual nucleotide solutions were 25 and 50 mM in nucleotide and 100 mM in $NaClO_4$, or 4 mM sodium cacodylate ($NaAs(CH_3)_2O_2$). The DNA model solution was prepared by dissolving the four 5'-ribonucleotides (20 mM G, 20 mM C, 30 mM A, 30 mM U) in 50 mM $NaNO_3$ [3].

Calf thymus DNA (PL Biochemicals, Milwaukee, WI) was purified by phenol extraction followed by ethanol precipitation. The DNA was dissolved in 4 mM sodium cacodylate (pH 7.9). The determination of the pH dependence of the Raman band of cacodylate at approx. 600 cm^{-1} against the 932 cm^{-1} band of perchlorate permitted the use of the cacodylate band as a frequency standard. For each experiment, the pH was adjusted by using either HCl or NaOH solutions. The pH was measured with a Radiometer PHM 64 pH meter and a combination electrode. The concentration of the DNA stock solution was 12.1 mM as determined by ultraviolet spectroscopy at 260 nm, $a_p = 6600$ cm^2/mol P [20]. Nucleotide solutions were filtered through 0.22 μm Millipore filters to remove particulates that would cause Tyndall scattering.

2.2. Spectra

All Raman spectra were obtained using the 514.5 nm excitation line from a Coherent Radiation CR52 argon ion laser. Argon plasma lines were dispersed with a prism monochromator. Laser power at the sample was approx. 500 mW. The Raman spectrometer system is based on a Spex industries Model 1400 double-monochromator to reject stray light and an RCA 31034 photomultiplier operated at 1700 V in a Products for Research housing cooled to −20°C. The spectrometer data acquisition was controlled by a Data General Nova II minicomputer. Spectral data were recorded on floppy disk and processed using Nova II software. Spectra presented in this report as Raman spectra were formed by the subtraction of solvent background. All spectra were collected in 1 cm^{-1} steps between 450 and 1850 cm^{-1}. The DNA spectra were stepped at 20-s intervals, whereas nucleotide spectra were stepped at 10-s intervals (acidic) or 2.55-s intervals (basic). Further information on the Raman instrument is presented in ref. [21].

3. Results and discussion

3.1. Acid region

Each nucleotide has one or more unique bands which can be used to follow protonation. The difference spectra for protonation are shown in fig. 1 and catalogued in table 1 for 5'-CMP, 5'-AMP and 5'-GMP. The protonation sites are shown in scheme 1. There are no changes in the ring vibrations of 5'-UMP or 5'-dTMP between pH 7 and 1. The features at about 970 cm^{-1} in all the difference spectra in fig. 1 are the result of protonation of the phosphate, $pK_a = 5.92–6.3$ [22]. The distinguishing feature in the Raman difference spectrum of N(3) protonation of the cytosine ring, $pK_a = 4.24$ [22], is the intense positive band at 1255 cm^{-1}, which is predominantly single bond in character [23–25]. The most prominent effects indicating protonation at the N(1) of 5'-AMP, $pK_a = 3.80$ [22], are three negative features between 1300 and 1400 cm^{-1} and two negative bands at 1479 and 1590 cm^{-1} which are the result of ring atom vibrations [23–25]. The most significant indications of 5'-GMP protonation, $pK_a = 2.3$ [22], are four negative Raman difference spectrum bands, two between 1300 and 1400 cm^{-1} and two at 1485 and 1578 cm^{-1} [23–25].

We then analyzed the protonation of a model system (spectra in fig. 2) with a base composition similar to that of calf thymus DNA. Ribonucleotides were substituted for deoxyribonucleotides, since the sugar bands do not distinctly change the spectrum of the base bands [32]. Also, 5'-UMP was used instead of 5'-TMP (5-methyluridylic acid), because the similar structure and pK_a values [22] result in similar protonation effects; the ring

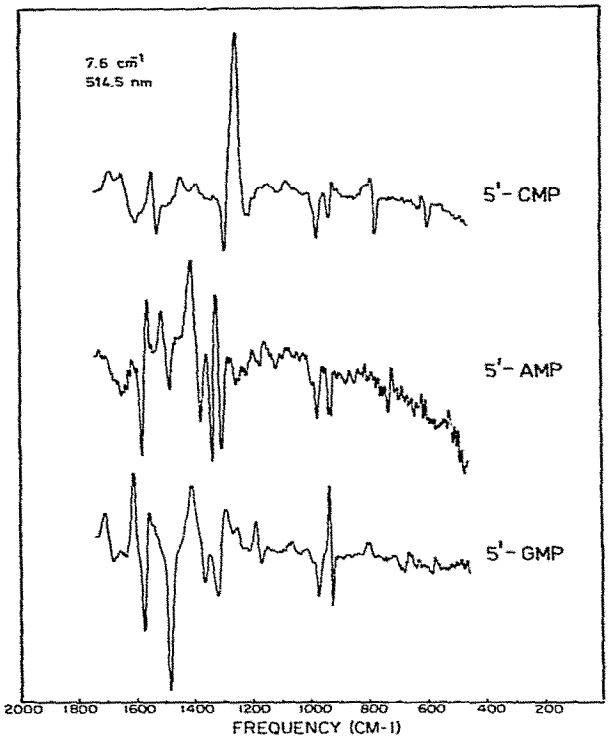

Fig. 1. Raman difference spectral protonation fingerprints for 25 mM solutions of 5'-CMP, 5'-AMP and 5'-GMP. These spectra were formed by subtraction of the spectrum at pH 7 from that at pH 1 of the same nucleotide. The spectra have been subjected to two-cycle 17-point quartic smoothing. The sharp derivative features of 5'-CMP and 5'-AMP at about 930 cm^{-1} are the result of an unmatched perchlorate concentration. Further experimental details are presented in the text. Frequencies are given in table 1.

Table 1

Raman frequences (cm^{-1}) for the pH-dependent Raman difference spectra of 5'-CMP, 5'-AMP and 5'-GMP in acidic solution

The data in this table are associated with fig. 1. The Raman difference spectrum was formed by subtracting the spectrum at pH 7 from that at pH 1.

5'-CMP	5'-AMP	5'-GMP
Peaks		
–	–	577
618	–	–
–	–	666
–	719	–
743	–	–
–	–	806
1081	1072	1064
–	1154	–
–	1197	1189
1255	–	–
–	1281	–
–	–	1295
–	1322	–
–	1356	1348
1391	–	–
–	1408	–
–	–	1410
1444	–	–
–	1511	–
1544	–	–
–	1558	1556
–	1613	1611
1694	–	–
Valleys		
596	–	–
–	–	681
–	730	–
778	–	–
977	976	975
1212	–	–
1285	1305	–
–	1337	1320
–	1377	1365
–	1481	1485
1527	–	–
–	1579	1574

nitrogens in uracil and thymine are not further protonated between pH 7 and 1. Fig. 3 shows the profile of the percent protonated species as a function of pH and also indicates the pH values at which the Raman spectra of the model system were recorded.

The Raman difference spectra of the model system follow the anticipated protonation order based on pK_a values of the individual nucleotides (fig. 3) [22]. Also, most of the major base bands of 5'-AMP and 5'-GMP in the Raman difference spectra show a decrease in intensity at pH 4.8 as a result of a decrease in the phosphate charge from −2 to −1 which facilitates base stacking and the associated Raman hypochromism [26–28]. The fact that base stacking is not observed for 5'-UMP is not surprising because even in poly(U) only

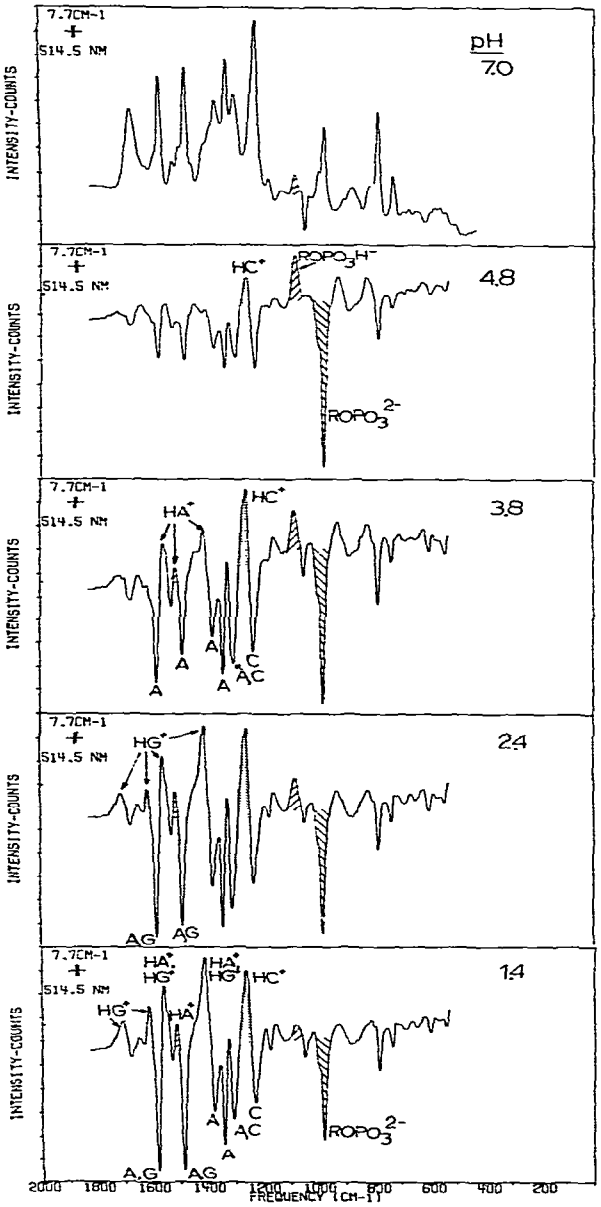

Fig. 2. Raman difference spectra of the 100 mM total phosphate calf thymus DNA model system in the acidic region. Referenced against 50 mM $NaClO_4$. The top spectrum is the Raman spectrum of the model system at pH 7.0. The Raman difference spectra were formed by subtracting the spectrum at pH 7.0 from those at lower pH. Spectra were subjected to two-cycle 25-point quadratic smoothing. Further details are available in the text.

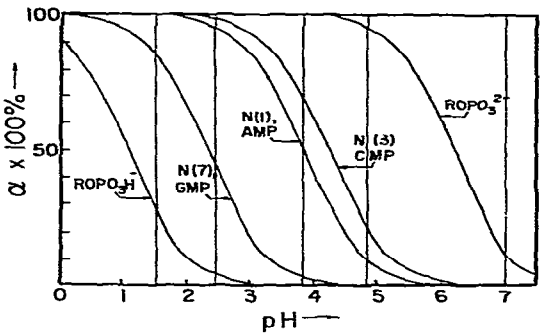

Fig. 3. Percent species distribution for protonation in the acidic range for 5'-CMP, 5'-AMP and 5'-GMP. These curves were constructed from data in ref. [22]. The vertical lines represent the pH values where model system spectra were obtained.

minimal base stacking is noted [27,29].

The spectra of calf thymus DNA between pH 10.5 and 5.0 are essentially identical. The spectra in fig. 4 show protonation when bands in the pH 5.54 and 4.09 spectra are compared to those at 1252 and 1300 cm^{-1}. The Raman difference spectra in fig. 5 show a doublet with one peak at 1259 cm^{-1} and less intense negative features at 1300, 1338, 1373, 1486 and 1574 cm^{-1} which indicate protonation of cytosine and adenine residues between pH 5.54 and 4.09. Cytosine protonation is suggested by the relative intensity plot of the 1252 cm^{-1} band in fig. 6a. The plots in fig. 6b and c show that H^+ binds to adenine as reflected in the 1335, 1373 and 1476 cm^{-1} intensity changes between pH 5.0 and 4.0. The intensity decrease of the 1476 cm^{-1} band below pH 3 in fig. 6c is the result of H^+ binding to the N(7) of guanine residues.

The midpoint of the intensity versus pH curves (defined as an apparent pH_m) suggests an order to the protonation. Apparent pH_m values were used, since in several cases the limiting values of relative intensity were not attained. Table 4 shows that adenine and cytosine residues are protonated first, followed by guanine residues below pH 3. Moreover, the Raman difference spectra demonstrate that H^+ binds to the same sites as in the mononucleotides.

Raman spectroscopy can monitor base stacking phenomena in addition to base protonation [4–12].

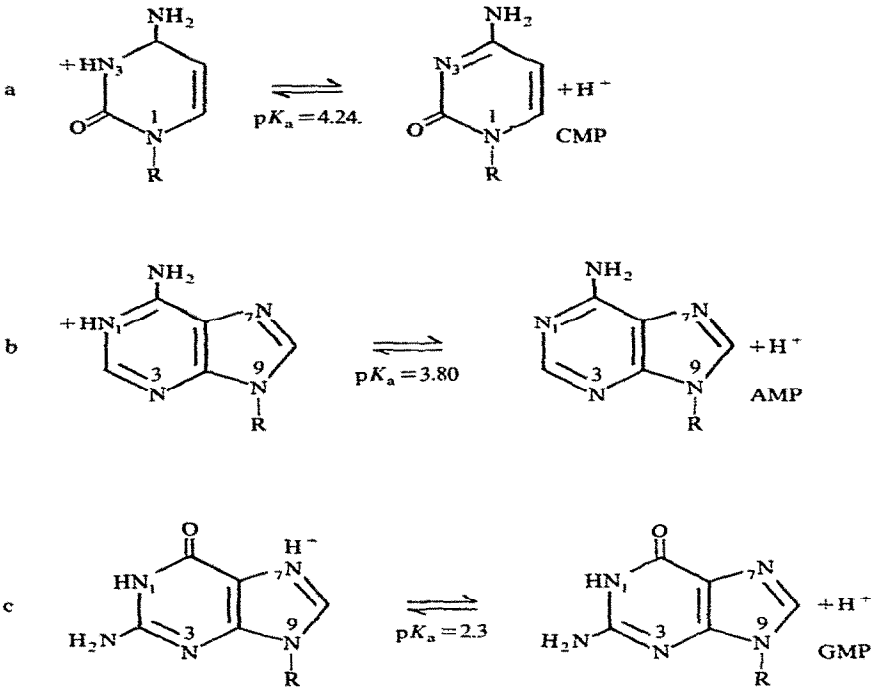

Scheme 1.

The base unstacking of adenine residues begins in the region where adenine protonation occurs as indicated by the band intensity changes at 721 cm^{-1} (fig. 6b). The intensity of the bands at 1335 and 1373 cm^{-1} does not increase above pH 3.5. The reasons for the initial decrease, followed by the increase in intensity for the 1335 and 1373 cm^{-1} bands, is that those bands are diagonostic of protonation and base stacking. H^+ binding to the N(1) of adenine results in a decrease in the intensity of the bands at 1335 and 1373 cm^{-1} (vide supra, fig. 1). Raman hypochromism, however, causes the intensity of the 1335 and 1373 cm^{-1} bands to increase [28]. The 721 cm^{-1} band intensity is not affected by protonation [25], but is hypochromic [27,28], therefore, only an increase in the band intensity is observed. Base stacking in cytosine residues can be tracked by examining the 783 cm^{-1} band in fig. 6a which does not vary in intensity on protonation of the monomer system [24]. The pH_{m2} value of 3.3 ± 0.1 for bands at 721, 747 and 783 cm^{-1} suggests a loss of base stacking for adenine, thymine and cytosine residues, respectively. The reduction in base stacking reflects the denaturation point of the double-stranded DNA. The increases in intensity over a broad pH range (≈ 2 pH units) imply an unstacking of the bases which resembles the premelting effects which are observed in the analysis of the thermal denaturation of DNA [5,6].

Raman spectra can also follow changes in the phosphate which are sensitive to variation in the backbone conformation [7,9]. The Raman spectra in fig. 4 indicate that the 835 cm^{-1} band, reflecting the B-conformation of DNA, virtually disappears in the pH 4.09 spectrum. The Raman spectra in fig. 4 suggest that the decrease in intensity at 835 cm^{-1}, characteristic of DNA in the B-conformation, may be coupled with an increase in intensity at 879 cm^{-1}. The increase in intensity of

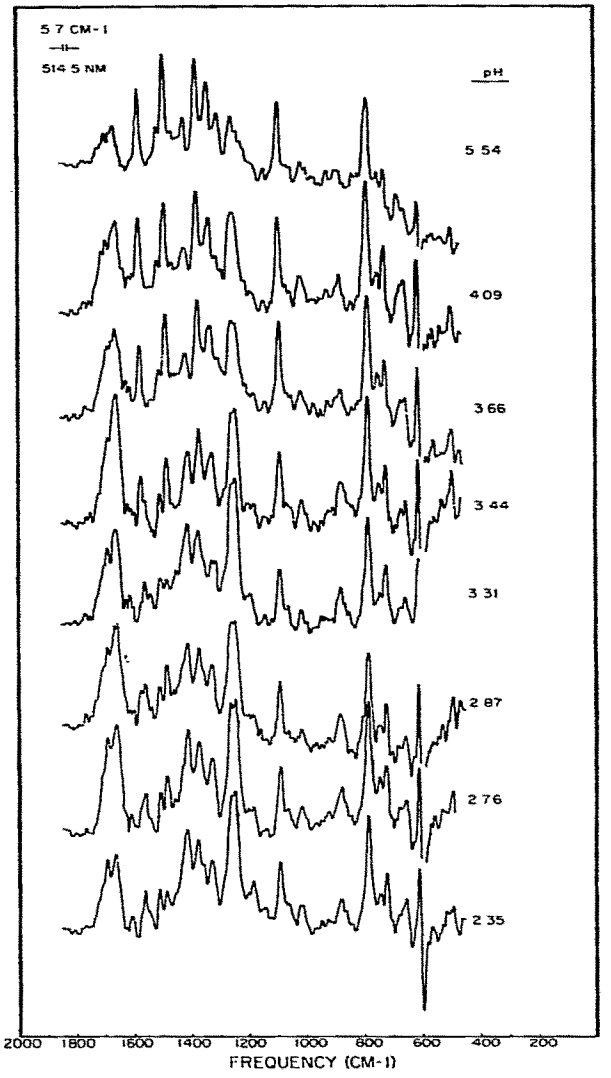

Fig. 4. pH-dependent Raman spectra of 12.1 mM total phosphate calf thymus DNA below pH 7.0. The spectra were formed by subtraction of a 4 mM sodium cacodylate solution (pH 7.42) from the spectra at lower pH. Spectra were subjected to one-cycle 25-point quartic smoothing with a cubic polynominal background subtraction. Further experimental details appear in the text. Frequencies are given in table 2.

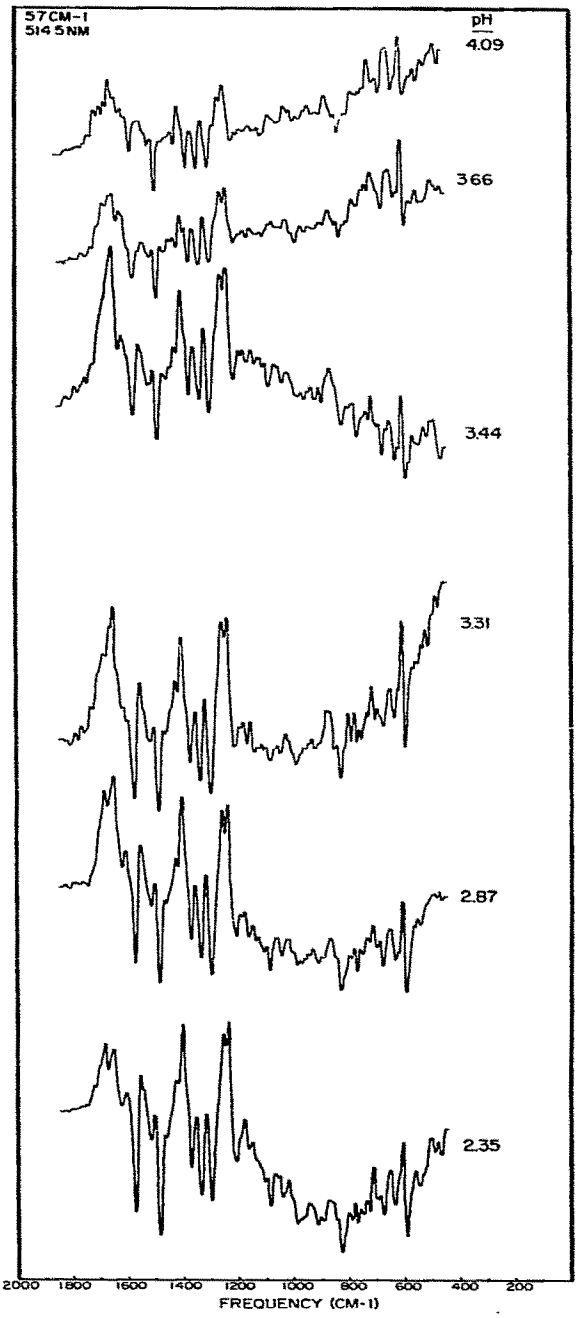

Fig. 5. pH-dependent of 12.1 mM Raman difference spectra of 12.1 mM calf thymus DNA in the acidic region. Spectra were formed by subtraction of the Raman spectrum at pH 5.54 from those at lower pH. The spectra were subjected to two-cycle 25-point quartic smoothing. Further experimental details appear in the text. Frequencies are given in table 3.

Table 2

Raman frequencies (cm^{-1}) Raman for the pH-dependent spectra of calf thymus DNA

The data in this table are associated with figs. 4 and 8. Raman difference spectra were formed by subtracting the solvent spectrum at pH 5.54 from the spectrum of interest.

pH		
2.35	5.54	11.87
–	467 w	–
493 m	–	–
–	–	504 m
–	–	534 m
–	555 w	553 m
566 w	–	–
–	–	639
655 m	–	–
–	689	676 m
721 m	726 m	723 m
747 m	747 m	–
783 vs	782 vs	782 vs
879 m	–	–
–	893 m	–
–	922 m	–
1012 m	1012 m	1010 m
–	–	1066 m
1089 s	1089 s	1086 s
1140 w	1140 w	1134 w
1182 w	–	–
1244 vs	–	1241 s
–	1252 s	–
1259 vs	–	–
–	1300 s	1301 vs
–	1335	–
1327 s	–	–
–	–	1350 vs
1373 vs	1373 vs	1374 vs
1409 vs	–	–
–	1417 m	1417 m
1484 vs	1468 vs	–
–	–	1476 vs
1508 m	–	1503 m
1558 m	–	–
–	1574 s	1576 s
1603 w	–	–
1658 s	1659 m	1652 s

the latter band appear to correspond to a C-type conformation of DNA, since the C-form DNA has bands between 865 and 890 cm^{-1} [7]. The formation of the C-type DNA may be the result of an overall decrease in the charge of the polynucleo-

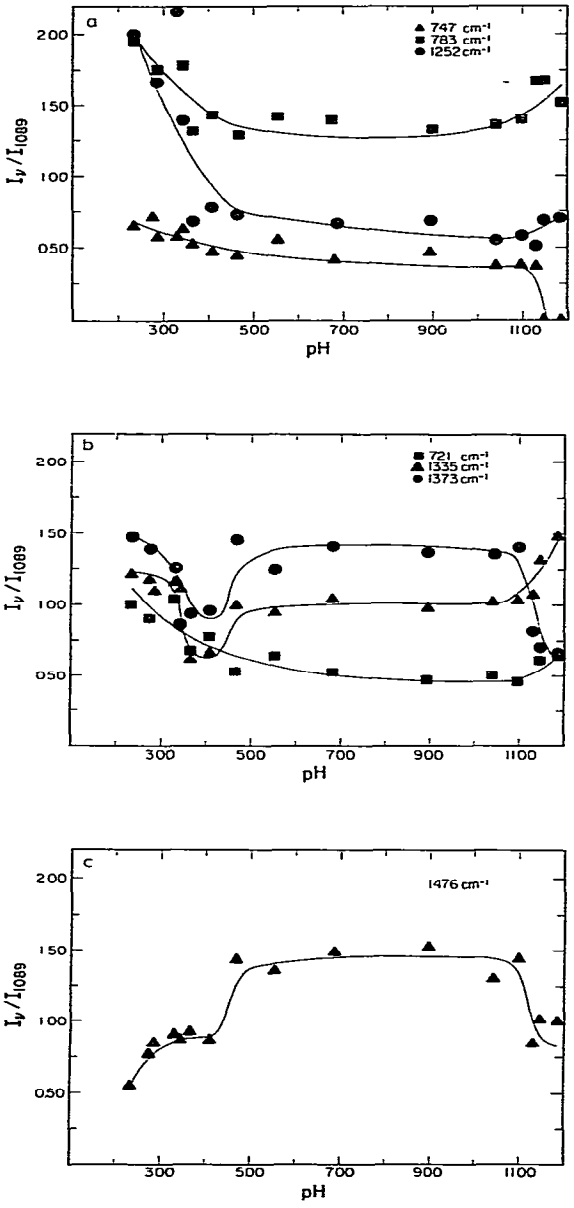

Fig. 6. Plots of relative intensity versus pH for calf thymus DNA. The plots were constructed from spectra in figs. 4 and 8 by referencing against the 1089 cm^{-1} phosphate band. (a) ▲, 747 cm^{-1} (T); ■, 783 cm^{-1} (C); ●, 1252 cm^{-1} (C); (b) ■, 721 cm^{-1} (A); ▲, 1335 cm^{-1} (A, G); ◐, 1373 cm^{-1} (A, G); (c) ▲, 1476 cm^{-1} (G, A).

Table 3

Raman frequencies for the pH-dependent Raman difference spectra of calf thymus DNA

The data in this table are associated with figs. 5 and 9. The Raman difference spectra were formed by subtracting the calf thymus DNA spectrum at pH 5.54 from the spectrum of interest.

pH 2.35	pH 11.78
Peaks	
482 w	–
507 w	508 m
565 w	558 w
–	600 m
–	645 w
656 m	–
717 m	–
739 w	–
–	765 m
783 w	–
	799 m
872 m	–
–	904 w
946 m	946 w
1023 w	1023 w
1071 m	1068 w
–	1102 w
–	1133 w
–	1158 m
1181 s	–
–	1203 vw
1241 vs	1249 m
1259 vs	–
–	1267 m
–	1307 vs
1320 s	–
1355 s	1349 vs
1405 vs	1405 m
–	1449 w
–	1473 m
1505 w	1505 vw
–	1527 w
1556 s	–
–	1590 vs
1607 w	–
1653 m	1654 m
1685 m	–
–	1739 m
Valleys	
–	746 m
–	774 w
831 m	–
1089 m	–
1300 s	–
1338 s	1333 s
1373 s	1374 s
–	1419 m
1486 vs	1490 s
1574 vs	1572 m
–	1675 m

tide chains; protonation permits closer approach of the phosphates [31].

3.2. Basic region

The difference spectra for deprotonation of 5'-GMP and 5'-TMP are shown in fig. 7 and catalogued in table 5. The deprotonation sites are shown in scheme 2. There are no changes in the ring vibrations of 5'-CMP and 5'-AMP between pH 7 and 12. The removal of an H^+ from 5'-GMP, $pK_a = 9.38$ [22], is best characterized by the bands between 1300 and 1400 cm^{-1} and the negative features at 1489 and 1573 cm^{-1}. The deprotonation of 5'-TMP, $pK_a = 10.0$ [30], is most easily distinguished by the negative features at 1378 and 1684 cm^{-1}, which detect changes in ring nitrogen and carbonyl vibrations, respectively [23].

The spectra in figs. 8 and 9 are examples of Raman and Raman difference spectra for calf thymus DNA above pH 7. We analyzed the spectra similarly to the method of the acidic region, i.e., by separating deprotonation, base stacking and backbone conformation. The Raman spectra of calf thymus DNA between pH 7.0 and 11.0

Table 4

Apparent transition pH values (pH_m) for calf thymus DNA

Data from fig. 6a–c were used to construct the table.

Band (cm^{-1})	$pH_{m,1}$	$pH_{m,2}$	$pH_{m,3}$	$pH_{m,4}$
721	–	3.4	–	11.6
747	–	3.3	–	11.4
783	–	3.3	–	11.4
1252	–	3.4	–	11.2
1335	–	3.5	4.2	11.3
1373	–	3.2	4.1	11.2
1476	2.6	–	4.1	11.1

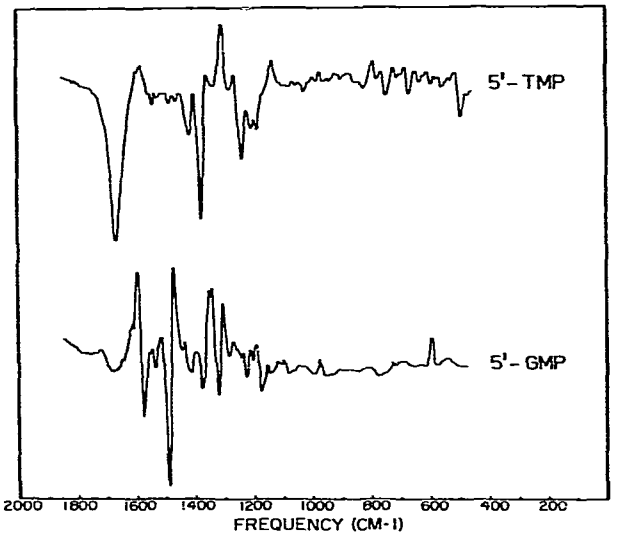

Fig. 7. Raman difference fingerprint spectra for deprotonation of 50 mM 5'-TMP and 5'-GMP. These spectra were formed by subtraction of the spectrum at pH 8 from that at pH 12 of the same nucleotide. The spectra have been subjected to two-cycle 17-point quartic smoothing. Further experimental details appear in the text. Frequencies are given in table 5.

showed little variation, as evidenced by the spectra in fig. 8 and the plots in fig. 6a–c. At pH values of approx. 11.0, however, intensity variations are observed (fig. 6a–c). Bands at approx. 1252 (partial thymine character) and 1476 cm^{-1} (guanine character) reflect H^+ removal from ring nitrogens at the N(3) of thymine and the N(1) of guanine. The data from the plots in fig. 6a and c and the spectra in fig. 8 suggest that guanine may be deprotonated at slightly lower pH values than thymine.

The bands at 721 and 783 cm^{-1} are diagnostic for base stacking in adenine and cytosine residues, respectively (vide supra). The increase in intensity observed in figs. 6a and b for those two bands was consistent with base unstacking paralleling base deprotonation. Therefore, the basic denaturation of calf thymus DNA proceeds by initial guanine deprotonation followed closely by thymine deprotonation and is coupled with a decrease in base stacking.

The amount of DNA in the B-conformation (fig. 9) between pH 11.00 and 11.87 is not known, but there is a possibility that a significant percentage of the DNA is still in the B-form at pH 11.87. However, there seems to be some change in the backbone conformation which we are not able to discern readily.

4. Conclusions

The acid pH denaturation of calf thymus DNA proceeded in at least two steps. The first step involves the protonation of adenine and cytosine

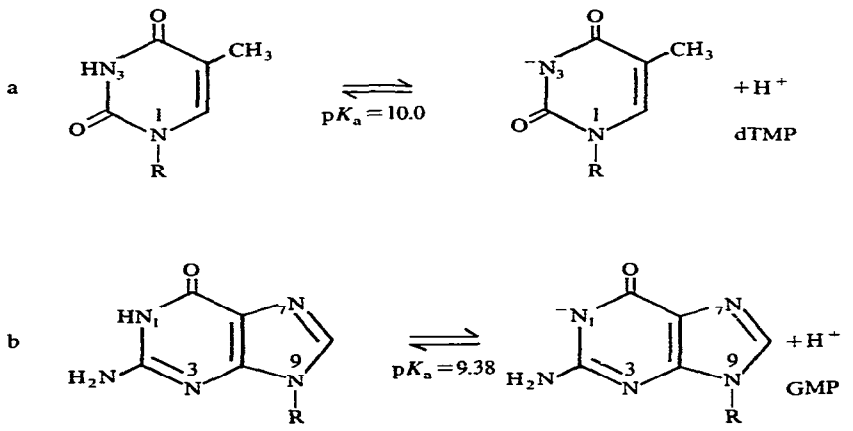

Scheme 2.

Table 5

Raman frequencies for the pH-dependent Raman difference spectra of 5'-GMP and 5'-TMP in basic solution

Data in this table are associated with fig. 7. The Raman difference spectra were formed by subtracting the spectrum at pH 8 from that at pH 12.

5'-GMP	5'-TMP
Peaks	
–	518
–	609
–	650
–	684
–	725
–	766
–	791
976	975
1037	–
1119	–
–	1137
1191	–
–	1264
–	1308
1304	–
1341	–
–	1360
1394	1402
1471	–
1515	–
1593	–
–	1582
Valleys	
–	497
–	670
–	749
–	782
–	1000
1174	–
–	1187
–	1212
1226	–
–	1241
1318	–
1374	1378
–	1420
1480	–
1573	–
–	1668
1673	–

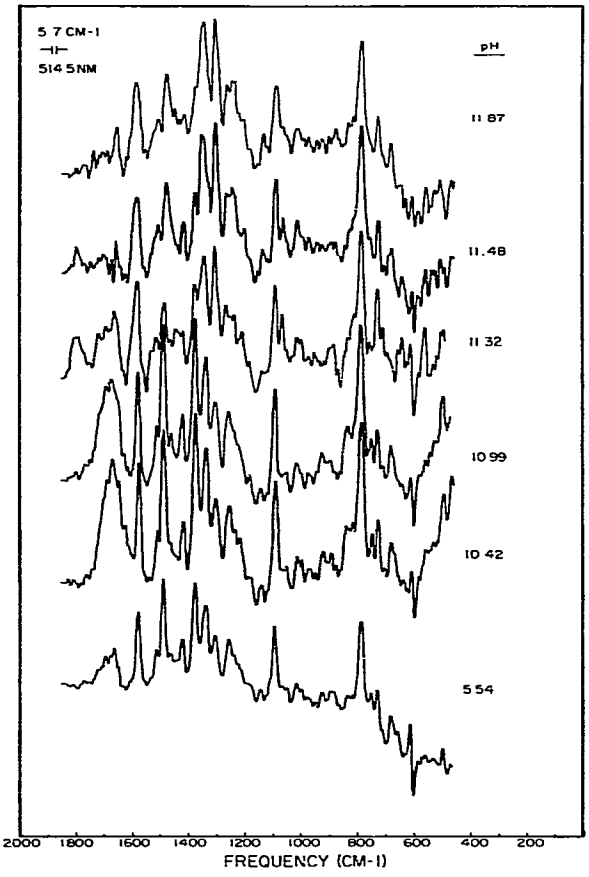

Fig. 8. pH-dependent Raman spectra of 12.1 mM calf thymus DNA above pH 7. These spectra were formed by the subtraction of the 4 mM sodium cadodylate (pH 7.42) spectrum from those at higher pH. Spectra were subjected to one-cycle 25-point quartic smoothing with a cubic polynomial background subtraction. Further experimental details appear in the text. Frequencies are given in table 3.

residues (pH 4.1) and the formation of C-type DNA. The second step is the actual denaturation at pH 3.3. Below the denaturation pH the guanine residues are protonated. Therefore, although the pH titration determined by ultraviolet spectroscopy shows behavior similar to that of premelting, the structural correlations are not as directed compared to those from Raman spectroscopy [19]. Raman spectroscopy indicates that several steps are involved in acidic denaturation of DNA. The reason that at least two steps are detected using Raman spectroscopy is that Raman spectroscopy

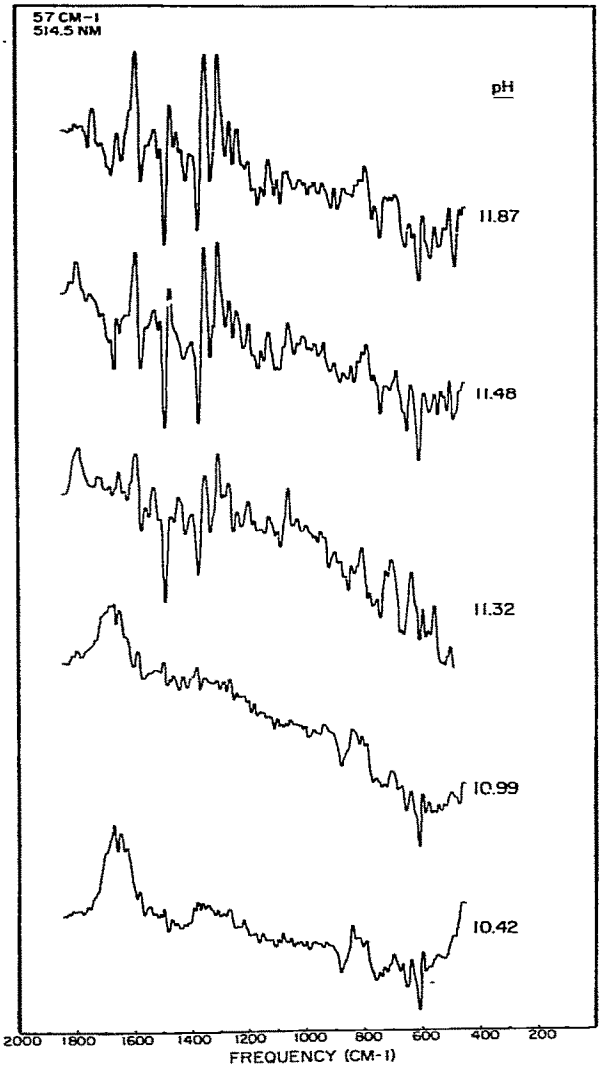

Fig. 9. pH-dependent Raman difference spectra of 12 mM calf thymus DNA. Spectra were formed by subtraction of the calf thymus DNA spectrum at pH 5.54 from those at higher pH. Spectra were subjected to two-cyle 25-point quartic smoothing. Further experimental details appear in the text. Frequencies are given in table 3.

is able to follow the binding of H^+ to bases, as well as base stacking and conformation; whereas ultraviolet spectroscopy provides more information on base stacking than on base protonation [19].

The alkaline pH denaturation of calf thymus DNA, in contrast to the acid denaturation, occurs over a very narrow pH range. Deprotonation occurs initially for guanine residues followed by thymine. Although these two changes in base deprotonation are coupled to a change in conformation, the B-conformation does not totally disappear.

Acknowledgements

This work was supported by funds provided through the National Institutes of Health Grant AM16101 and National Cancer Institute Postdoctoral Fellowship No. CA 03254-02 (S.M.). The comments of the referee were greatly appreciated in the final preparation of this manuscript.

References

1 R.S. Tobias, T.H. Bushaw and J.C. English, Indian J. Pure Appl. Phys. 16 (1978) 401.
2 R.W. Chrisman, S. Mansy, H.J. Peresie, A. Ranade, T.A. Berg and R.S. Tobias, Bioinorg. Chem. 7 (1977) 245.
3 G.Y.H. Chu, S. Mansy, R.E. Duncan and R.S. Tobias, J. Am. Chem. Soc. 100 (1978) 593.
4 R.J. Douthart, S. Mansy, R.V. Schär, T. O'Connor and R.S. Tobias, submitted for publication.
5 L. Rimai, V.M. Maher, D. Gill, I. Salmeen and J.J. McCormick, Biochim. Biophys. Acta 361 (1974) 155.
6 S.C. Erfurth and W.L. Peticolas, Biopolymers 14 (1975) 247.
7 a. S.C. Erfurth, E.J. Kiser and W.L. Peticolas, Proc. Natl. Acad. Sci. U.S.A. 69 (1972) 938; b. D.C. Goodwin and J. Brahms, Nucleic Acid Res. 5 (1978) 835.
8 M. Zama, D.E. Olins, B. Prescott and G.J. Thomas, Jr, Nucleic Acid Res. 5 (1978) 3881.
9 S.C. Erfurth, P.S. Bond and W.L. Peticolas, Biopolymers 14 (1975) 1245.
10 G.J. Thomas, Jr and K.A. Hartman, Biochim. Biophys. Acta 312 (1973) 311.
11 G.J. Thomas, B. Prescott, P.E. McDonald-Ordzie and K.A. Hartman, J. Mol. Biol. 102 (1976) 103.
12 E.B. Brown and W.L. Peticolas, Biopolymers 14 (1975) 1259.
13 M.T. Record, Jr, Biopolymers 5 993 (1967).
14 W.F. Dove, A. Wallace and N. Davidson, Biochem. Biophys. Res. Commun. 1 (1959) 312.
15 L.G. Bunville, E.P. Geiduschek, M.A. Rawitscher and J.M. Sturtevant, Biopolymers (1965) 213.
16 C. Zimmer and H. Venner, Biopolymers 4 (1966) 1075.

17 C. Zimmer, G. Luck, H. Venner and J. Fric, Biopolymers 6 (1968) 563.
18 R.E. Chapman, Jr and J.M. Sturtevant, Biopolymers 9 (1970) 445.
19 Y. Coortois, P. Fromageot and W. Guschlbauer, Eur. J. Biochem. 6 (1968) 493.
20 H.R. Mahler, B. Kline and B.D. Mehrotra, J. Mol. Biol. 9 (1964) 801.
21 R.W. Chrisman, J.C. English and R.S. Tobias, Appl. Spectrosc. 30 (1976) 168.
22 R.M. Izatt, J.J. Christensen and J.H. Rytting, Chem. Rev. 71 (1971) 439.
23 R.C. Lord and G.J. Thomas, Jr, Spectrochim. Acta 23A (1967) 2551.
24 T. O'Connor, C. Johnson and W.M. Scovell, Biochim. Biophys. Acta 447 (1976) 484.
25 T. O'Connor, C. Johnson and W.M. Scovell, Biochim Biophys. Acta 447 (1976) 495.
26 P.C. Painter and J.L. Koenig, Biopolymers 15 (1976) 241.
27 E.W. Small and W.L. Peticolas, Biopolymers 10 (1971) 69.
28 B.L. Tomlinson and W.L. Peticolas, J. Chem. Phys. 52 (1970) 2154.
29 E.G. Richards, C.P. Flessel and J.R. Fresco, Biopolymers 1 (1963) 431.
30 R.O. Hurst, A.M. Marko and G.C. Butler, J. Biol. Chem. 204 (1953) 847.
31 D.A. Marvin, M. Spencer, M.H.F. Wilkins and L.D. Hamilton, J. Mol. Biol. 3 (1961) 547.
32 E.W. Small and W.L. Peticolas, Biopolymers 10 (1971) 1377.